

Adsorption/desorption behavior of cationic dyes on Moroccan clay: equilibrium and mechanism

A. Bennani Karim*^{1,2}, B. Mounir¹, M. Hachkar¹, M. Bakasse³, A. Yaacoubi²

¹The team of research Analysis, Checks and Environment, High School of Technology, University Cadi Ayyad, BP 89, Safi, Morocco

²The team Environmental and Experimental Methodology, Laboratory of Applied Organic Chemistry, Faculty of Sciences Semlalia, PO Box 2390, Marrakech, Morocco.

³The team of Analysis of the Microphones Polluting Organic, Faculty of the Sciences, University Chouaib Doukkali, BP 20, El Jadida, Morocco.

Received 01 Jul 2016,
Revised 09 Nov 2016,
Accepted 14 Nov 2016

Keywords

- ✓ Basic dyes,
- ✓ Moroccan clay,
- ✓ Adsorption,
- ✓ desorption,
- ✓ thermodynamic parameters,
- ✓ IR spectrum.

asmaabennani@yahoo.fr

Abstract

Moroccan clay were prepared and tested as adsorbent for removal of three basic dyes: Basic Red 46 (BR46), Methylene Blue (BM) and Green Malachite (GM) from aqueous solution. The adsorption kinetic was studied, the experimental data isotherms were analysed using the Langmuir, Freundlich and Redlich Peterson models. Thermodynamical parameters (ΔH° , ΔS° , ΔG° , and E_a) were also calculated for the dyes adsorption onto clay, it revealed that the adsorption process is exothermic in nature for the BR46 dye. Nevertheless, it is endothermic for BM and GM. The E_a values for BR46, BM and GM are observed to be 40, 64 and 76 kJ/ mole, respectively. These results indicates that the adsorption has a low potential barrier for BR46 dye and assigned to a physisorption. Whereas, the chemical adsorption mechanism is occurred for the BM and the GM dye. The desorption of the basic dyes using NaCl and CaCl₂ at different salt dyes ratio onto raw clay samples were studied using a batch adsorption. Results showed that the presence of other ions (Na⁺ and Ca²⁺) reduces the dyes uptake onto clay and promote significantly the dyes desorption when the salt dye ratio is less than 1, Whereas, the desorption effect is limited when this ratio is more than 1. The adsorption mechanism has been confirmed by IR spectra decomposition.

1. Introduction

The textile industry plays an important role in the global economy of our life. It consumes large quantities of water both for finishing, fixing dyes on the substrate, and generating large amounts of waste waters, thus, the discharged effluents are highly altered by dyes [1]. Effluent treatment from dyeing and finishing processes in the textile industry is one of the most significant environmental problems [2]. Therefore, color removal from wastewater is very important for solving the ecological, biological and industrial problems associated with the dyes [3]. In effect, its oral consumption is toxic, hazardous and carcinogenic due to presence of nitrogen. It when discharged into receiving streams will affect the aquatic life and causes detrimental effects in liver, gill, intestine, gonads and pituitary gonadotrophic cells. In humans, it may cause irritation to the respiratory tract if inhaled and causes irritation to the gastrointestinal tract upon ingestion. Contact to cationic dyes as BR46 with skin cause irritation with redness and pain. Upon contact with eye will lead to permanent injury of human eyes and laboratory animals [4, 5].

Malachite green (GM) is a N-methylated diaminotriphenylmethane dye, which is most widely used for coloring purpose, amongst all other dyes of its category. This cationic dye is generally used for the dyeing of cotton, wool, silk, leather, jute, paper, and also widely used in distilleries for coloring purposes. It is also used as therapeutic agent (fungicide, ectoparasiticide) and as antiseptic, but only for external applications on the wounds and ulcers, however, its oral consumption is toxic, hazardous and carcinogenic due to presence of nitrogen. It when discharged into receiving streams will affect the aquatic life and causes detrimental effects in liver, gill, kidney, intestine, gonads and pituitary gonadotrophic cells. In humans, it may cause irritation to the respiratory tract if inhaled and causes irritation to the gastrointestinal tract upon ingestion. Contact to malachite green with skin cause irritation with redness and pain. Upon contact with eye will lead to permanent injury of human eyes

and laboratory animals [5]. It is known to be highly toxic to mammalian cells and to act as a tumour enhancing agent. However, despite the large amount of data on its toxic effects, MG is still used in aquaculture and other industries [5- 7]. Methylene blue dye is the most commonly used in the dyeing of cotton, silk and wood. It can create eye burns causing permanent damage to the eyes of man and animals. Its inhalation can lead to breathing difficulties by ingestion through the mouth which produces a burning sensation, nausea, vomiting, abundant and cold sweat [8]. In order to minimize the possible damages to human and environment arising from the effluents containing this dyes, various kinds of treatments technologies such as adsorption, chemical flocculation [9, 10], chemical oxidation, froth flotation, ultra filtration and biological treatment technologies have been employed [11]. Among these, adsorption is one of the popular methods for wastewater treatment on account of its easy and inexpensive operation [3]. The most common adsorbents reported for basic dyes removal from wastewater are perlite [6], chitosan bead [7] activated carbon [12], orange peel [13] and natural clay [14]. Clays are particularly attractive adsorbents, since these are easily available at low cost [11]. In the present study, experiments have been performed for the removal of BR46, BM and GM dyes using adsorption techniques. Moroccan crude clay has been selected as adsorbent and added to the solution containing dye. The effects of temperature, initial dye concentration, adsorption isotherms have been studied under stirred condition. The desorption efficiency was investigated by adding NaCl and CaCl₂ at different concentrations.

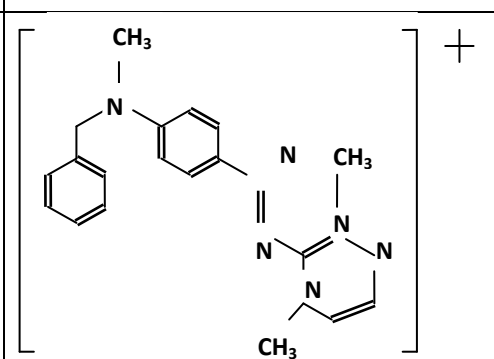
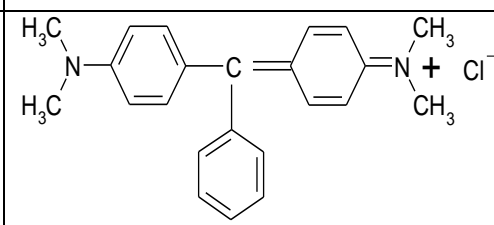
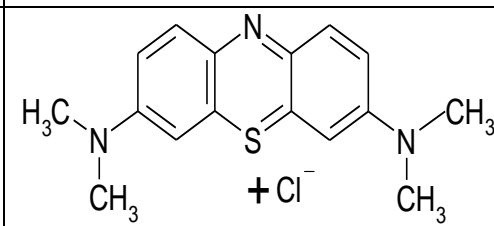
2. Materials and methods

2.1. Materiel

2.1.1. Adsorbate

Some characteristics of the basic cationic dyes used as adsorbates are summarized in table 1

Table 1: Some characteristics of the basic cationic dyes used as adsorbates

Adsorbat	Masse Molaire (g.mole ⁻¹)	Origine	λ_{max} (nm)	Structure
BR46	357,5	SDI textile company (Safi, Morocco)	532	
GM	463,5	SDI textile company (Safi, Morocco)	618	
BM	319,5	High School of Technology	666	

2.1.2. Adsorbent material

The raw adsorbent Moroccan clay used in this work is collected from a natural basin in the region of Safi (Morocco), crushed and sieved to $< 0,08 \mu\text{m}$ size fractions. Then, it was dried at 105°C for 24h and used for further experiments. The chemical composition of this clay is: 53,11 % SiO_2 , 16,95 % Al_2O_3 , 5,94 % Fe_2O_3 , 3,51 % CaO , 2,51 % MgO ; 0,2 % SO_3 ; 4,64 % K_2O ; 0,26% Na_2O ; 0,09 % P_2O_5 [15].

The mineralogical identification is performed by XRD in Siemens D500 diffractometer using a $106 \text{CuK}\alpha$ radiation ($\lambda = 1.5406 \text{ \AA}$) is produced under conditions of 40 kV and 20 mA, his predominant peaks are $9,99 \text{ \AA}$; $7,16 \text{ \AA}$; $4,25 \text{ \AA}$; $3,03 \text{ \AA}$ and $2,9 \text{ \AA}$ which correspond to illite, kaolinite, quartz, calcite and dolomite [15].

Fourier transform infrared spectroscopy (FTIR) of the adsorbent was obtained (and transformed to Microsoft Excel) by using an FTIR spectrophotometer (JASCO corp, FT/ IR 620 REV. 1.00.) to assess the different band attribution. About 100 mg KBr disks containing approximately 1% of clay samples was prepared shortly before recording the FTIR spectra in the range of $400\text{--}4000 \text{ cm}^{-1}$ and with a resolution of 4 cm^{-1} . The resulting spectra were the average of 30 scans.

2.2. Methods

2.2.1. Adsorption experiments

The adsorption experiments were carried out in stirred batch by varying dye concentration while the adsorbent clay was kept constant to 40 mg, which was used as optimal amount for further experiments in our earlier studies [15] in 100 mL dye solution. Samples of 3 mL of mixture were withdrawn from the batch at predetermined time intervals and the supernatant was centrifuged for 8 min at 2800 r.p.m. The dyes concentrations were determinate from their absorbance characteristics in the UV-Visible range. A spectrophotometer (GBC (Ajax, Ontario) UV/visible 911) was used for experiments. A linear correlation was established between the dye concentration and the absorbance at $\lambda_{\text{max}} = 532; 666$ and 618 nm for BR46, BM and GM respectively in the range $C_{\text{dye}} = 0\text{--}28 \text{ mg/L}$ with a coefficient of correlation $r^2 \sim 1$.

2.2.2. Sorption isotherms

The equilibrium isotherms are very important for understanding the adsorption systems. The variation of the dye concentration method, while keeping the same mass of the adsorbent, is used to calculate the adsorption characteristics of the adsorbent.

Preliminary experiments demonstrated that the equilibrium was established in 70 min for all the dyes. The sorption isotherms were established using adsorbent clay suspensions in BR46, BM and GM solutions (solid / solution ratio = 0.4 g/L used as optimal amount in our earlier studies [15] in a range from 10 to 28 mg/L at natural pH of 6. The suspensions were stirred during the equilibrium time at room temperature $\pm 22^\circ$, and then centrifuged. The dye concentration was determined as above.

2.2.3. Desorption studies

The desorption studies were carried out by studying the effect of the addition of salts (NaCl and CaCl_2). 50 mL of $0,003 \text{ M}$ of NaCl and $0,003 \text{ M}$ of CaCl_2 was added separately to 50 mL samples containing 40 mg of the clay fully loaded with initially $0,0006 \text{ M}$ of BR46, BM and GM separately. In effect, this amount of sodium and calcium electrolytes solutions were prepared and added to suspensions stirred until equilibrium with different molecular ratio of salt and dyes: 0.25; 0.5; 1; 2 and 5 in separate glasses, The suspensions were agitated for 60 min, then the supernatants were collected for analyses as follow: Samples of 3 mL of mixture were withdrawn from the batch at predetermined time intervals and the supernatant was centrifuged for 8 min at 2500 r.p.m. The desorbed dye concentrations were determinate from their absorbance characteristics in the UV – visible range. A spectrophotometer (GBC (ajax, ontario) UV/visible 911) was used for experiments. The salts NaCl and CaCl_2 used in these tests were of analytical grade, corresponding to a purity of 99%.

The adsorbent capacity is an important factor because it determines how much adsorbent is required to quantitatively remove a specific amount of metal ions from the solutions [16]

The amount of dye ion desorbed was obtained from the difference between the amount of dye ion fully loaded on the adsorbents and the amount of the same in solution. Reduced adsorption is calculated by the following equation:

$$\text{Desorption \%} = (q_0 - q_i / q_0) * 100 \quad (1)$$

Were q_0 is the maximum adsorption capacity in the absence of salts and q_i the maximum adsorption capacity in the presence of salts in a ratio R

2.2.4. Effect of temperature:

Temperature effect on adsorption for determination of thermodynamic parameters was studied for four temperatures: 30; 40; 50 and 60°C. A sample of 40 mg of clay was added to dyes solution (100 mL, 16 mg/l for the GM, 20 mg/L for the BR46 and 24 mg/L for the BM) at pH = 6. The experiments were carried out in a constant temperature shaker bath which controlled the temperature to within $\pm 1^\circ\text{C}$.

Arrhenius equation has been applied to evaluate the activation energy of adsorption representing the minimum energy that reactants must have for the reaction to proceed, as shown by following relationship:

$$\ln k_2 = \ln A - E_a / RT$$

Where k_2 is the rate constant obtained from the pseudo- second- order kinetic model, (g/mg. min), E_a is the Arrhenius activation energy of adsorption, (kJ/mole), A is the Arrhenius factor, R is the universal gas constant (8.314J/mole K) and T is the absolute temperature. When $\ln k_2$ is plotted against $1/T$, a straight line with slope of $- E_a/R$ is obtained [17].

3. Results and discussion

3.1. Characterization of adsorbent:

Table 2 shows the tabulated data for FTIR spectra band assignments for raw clay sample obtained from Fig. 1. In the range of 400 - 4000 cm^{-1} . As shown in Figure 1, the spectra display a number of absorption peaks, indicating the complex nature of the clay adsorbent examined. The FTIR spectroscopic analysis indicated broad bands at 3498 cm^{-1} , representing bonded OH groups, while the bands at 3614 cm^{-1} is associated with the stretching vibrations of hydroxyl groups which are coordinated to the octahedral magnesium and the tetrahedral silicon [18].

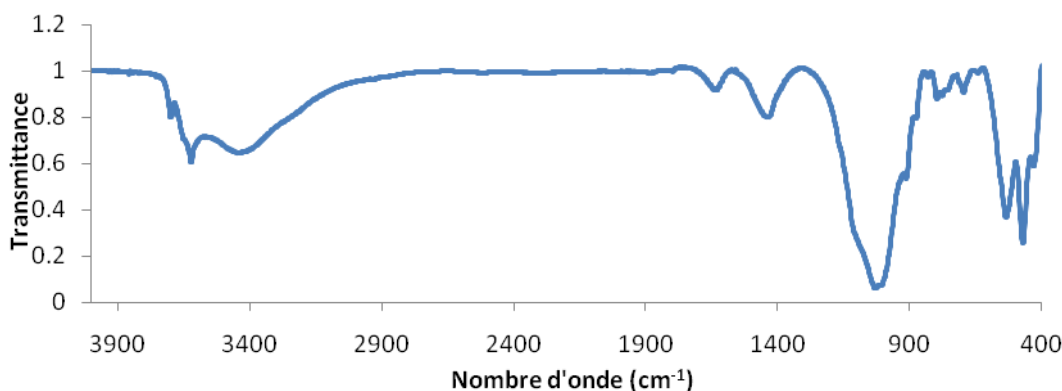


Figure 1: FTIR spectra of Safi Moroccan clay

The bands at 527 and 473 cm^{-1} corresponded to deformation vibrations of Si-O-Al and Al-OH, respectively. The bands at 3415 and 1651 cm^{-1} are attributed to adsorbed water and zeolitic water. The OH bending bands appear at 985 cm^{-1} [19].

The additional peaks at 1442 and 874 cm^{-1} , indicate the calcite CO group stretching vibration presence [20], while those at 2526; 1817 and 1450 cm^{-1} are related to dolomite bands, associated with the stretching vibration of the group CO_3^{2-} [20].

3.2. Adsorption isotherms

Adsorption isotherms describe qualitative information on the nature of the solute-surface interaction as well as the specific relation between the concentration of adsorbate and its degree of accumulation onto adsorbent surface at constant temperature.

Adsorption isotherms are critical in optimizing the use of adsorbents, and the analysis of the isotherm data by fitting them to different isotherm models is an important step to find the suitable model that can be used for design purposes [21]. Three models were tested to describe the adsorption experimental results: the Langmuir model, the Freundlich model and Redlich- Peterson model (R-P) which contains three parameters including features of Langmuir and Freundlich isotherm equations [22].

♦ Langmuir isotherm.

In 1918, Langmuir proposed a theory to describe the adsorption of gas molecules onto metal surfaces [23]. Langmuir's model of adsorption predicts the existence of monolayer coverage of the adsorbate at the outer

surface of the adsorbent. The isotherm equation further assumes that adsorption takes place at specific homogeneous sites within the adsorbent, which implies that all adsorption sites are identical and energetically equivalent.

Theoretically, the sorbent has a finite capacity for the sorbate. Therefore, a saturation value is reached beyond which no further sorption can occur [24]. The saturated or monolayer capacity can be represented as the known Langmuir equation:

$$q_e = q_{\max} * K_L * C_e / 1 + K_L * C_e \quad (2)$$

Where q_e is the equilibrium dye concentration on the adsorbent (mg g^{-1}), C_e is the equilibrium dye concentration in solution (mg dm^{-3}), q_{\max} is the monolayer capacity of the adsorbent (mg g^{-1}), and K_L is the Langmuir adsorption constant ($\text{dm}^3 \text{mg}^{-1}$)

Freundlich isotherm

The Freundlich equation [25] is an empirical equation employed to describe heterogeneous systems, characterized by the heterogeneity factor $1/n$, describes reversible adsorption, and is not restricted to the formation of the monolayer,

$$q_e = K_F C_e^{1/n} \quad (3)$$

Where q_e is the equilibrium dye concentration on adsorbent (mg g^{-1}), C_e is the equilibrium dye concentration in solution (mg dm^{-3}), K_F is Freundlich constant which indicates the sorption capacity of the sorbent. (mg g^{-1}), and $1/n$ is the heterogeneity factor.

Redlich and Peterson isotherm

Redlich and Peterson incorporated three parameters into an empirical isotherm. The Redlich- Peterson isotherm model combines elements from both the Langmuir and Freundlich equations [26] and the mechanism of adsorption is a hybrid one and does not follow ideal monolayer adsorption

$$q_e = K_R C_e / 1 + a_R C_e^b \quad (4)$$

Error analysis

The traditional approach of determining isotherm parameters is based on the linearized form of isotherm equation by best fitting the linearized isotherm equation to the experimental data. However, the correlation coefficient R^2 generated from this method has the drawback that it may not provide the best isotherm constants for correlating the original (non-linearized) isotherm equation with experimental data points. Because of the inherent bias from linearization, alternative isotherm parameters are determined by non-linear approach. The fitness of the isotherms, generated from non-linear approach, to the experimental data is optimized by error analysis. In this project, sum of squared error (SSE) (Eq. (5)) is employed and the isotherm parameters are determined by minimizing the SSE values across the entire concentration range of studies using the Solver add-in with Microsoft's spreadsheet, excel [22].

$$RMSE = \sqrt{\frac{\sum (q_{e_{\text{exp}}} - q_{e_{\text{cal}}})^2}{N}} \quad (5)$$

Where $q_{e_{\text{exp}}}$ is the experimental value of q_e (mg/g), $q_{e_{\text{cal}}}$ is the predicted value of q_e by models (mg/g). N indicates the number of data points in the experimental run

The amounts of adsorbed quantities of each dye at the equilibrium (q_e), versus equilibrium dye concentration were drawn in Fig. 2. The experimental adsorption obtained was compared with the adsorption isotherm models and the constants appearing in each equation of those models were determined by non-linear regression analysis. The results of this analysis are tabulated in Table 2. The square of the correlation coefficient (r^2) are also shown in this table.

Among the tested three-parameter equations, the better and perfect representation of the experimental results of the adsorption isotherms is obtained using the Redlich Peterson and the Langmuir models (Fig. 2). According to Table 2, the coefficients of correlation are near to 0.99.

The methylene blue and malachite green isotherms show an important adsorption with almost weak concentration in the solution, it is an isotherm of the type H in Giles classification [27]. Generally, Isotherms types H are the result of the dominance of strong ionic adsorbate-adsorbent interactions [28]. A chemical adsorption of positively charged functional groups of MB and MG on the negatively charged surface groups of the clays is proposed.

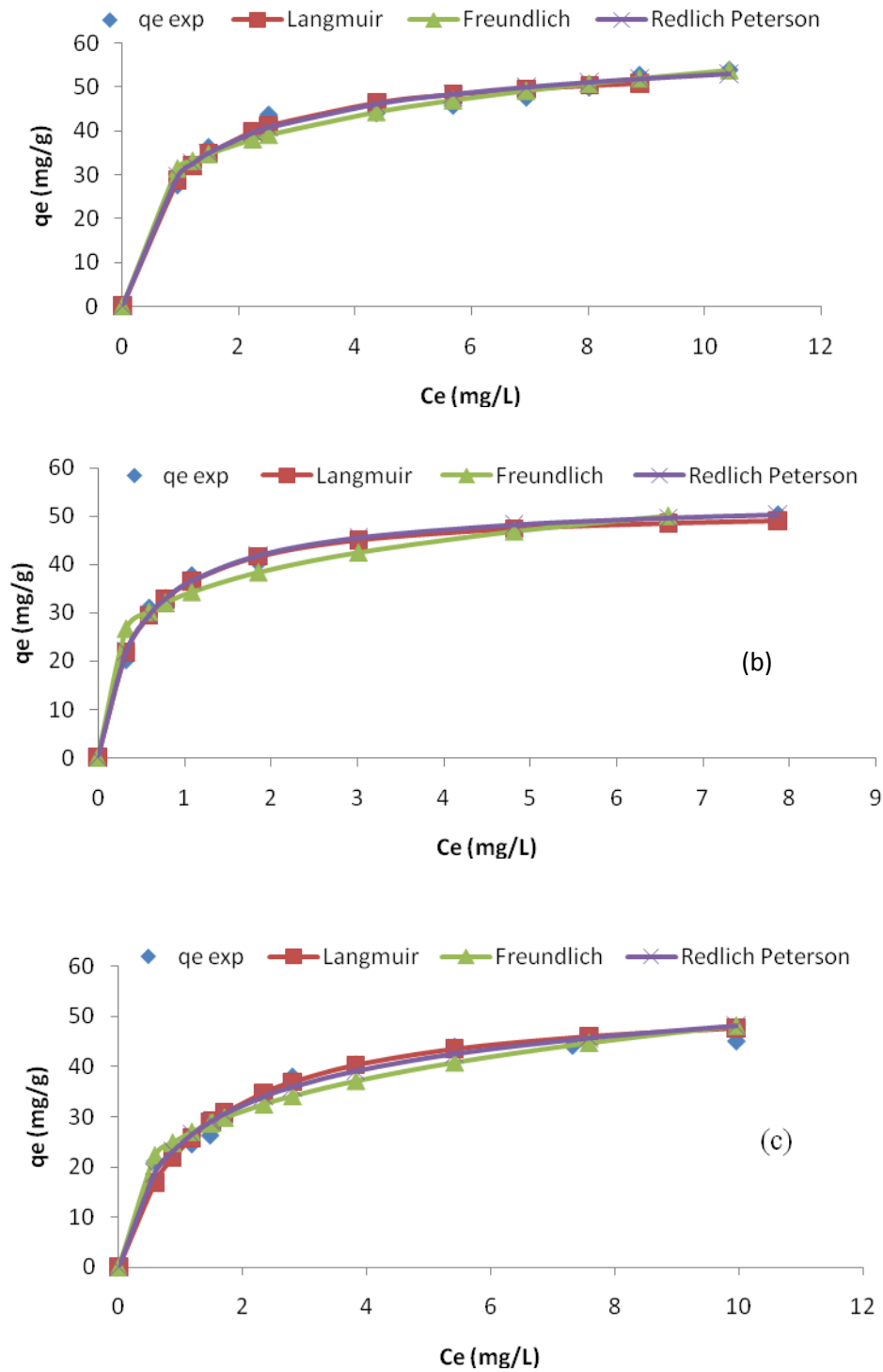


Figure 2: Adsorption isotherms of dyes (a): BR46 (b) BM and (c): GM (T° : $(25 \pm 2)^\circ\text{C}$, m_{clay} : 400 mg /L) onto clay

The values of the maximum adsorption capacity obtained using the Redlich Peterson equation are near than those calculated by the Langmuir and Freundlich models for the BR46 and the GM dyes, higher than the value calculated for the BM dye. The mean value of the average percentage error for the studied compounds is for the Redlich Peterson model than for the Langmuir and Freundlich models.

It can be also seen that the values of n at equilibrium are 4.04; 6.94 and 3.68 for the BR46, BM, and GM respectively. It is noted that the values of n are bigger than 1, reflecting the favourable adsorption [29].

Table 2: Isotherm parameters of the Langmuir, Freundlich and Redlich Peterson models obtained by using non-linear regression

Modèles d'isothermes	BR46	BM	GM
	Langmuir		
q_0 (mg/g)	54.14	50,29	53,78
q_0 (mmole/g)	0,12	0,16	0,12
K_L (L/mg)	1,19	3,26	0,78
R^2	0,99	0,96	0,98
R_L	0,27	0,24	0,23
Δq %	4	3.8	7.3
Freundlich			
K_F (mg/g)	30.50	36.90	25.78
n	4.04	6.94	3.68
R^2	0.96	0.95	0.97
Δq %	9	12.2	7.3
Redlich Peterson			
K_R (L.g ⁻¹)	52.88	219.22	65.44
a_R (L.mg ⁻¹)	0.80	4.76	1.66
α	1.08	0.95	0.88
R^2	0.99	0.96	0.98
Δq %	3.5	4.1	5.9

3.3. The temperature effect of BR46, BM and GM dyes onto clay

Evaluation of temperature was carried out with the scope of testing the ability of the clays in dyes removal in the case of different kinds of effluents, bearing in mind the specific circumstances of dye stuff wastes.

The quantities of BR46, MB and GM adsorbed on the clay as function of solution temperature are shown in Table 3. The table indicates that the increase in solution temperature increases the adsorbed quantities of BM and GM, which may be due to increase in dye mobility that may occur at high temperature between the adsorbent and the adsorbate [30]. However, the adsorbed quantity of BR46 decreases significantly with the increase in temperature. From these results, the thermodynamic parameters such as the standard changes in free energy (ΔG°), enthalpy (ΔH°) and entropy (ΔS°) were determined from the plot of $\log(K_C)$ versus $1/T$ [31]:

$$\ln K_c = -\Delta H^\circ_{\text{ads}}/RT + \Delta S^\circ_{\text{ads}}/R \quad (6)$$

Where R is the gas constant (8.314 J/ mol K), K_c is the equilibrium constant and T is temperature in K. The K_c value is calculated from Eq. (6):

$$K_c = q_e/C_e \quad (7)$$

Where q_e and C_e are the equilibrium amount adsorbed (mg/g) and equilibrium concentration (C_e in mg/L) at different temperatures (mg/L).

The change in standard free energy (ΔG°) can be calculated from the following equations:

$$\Delta G^\circ_{\text{ads}} = \Delta H^\circ_{\text{ads}} - T\Delta S^\circ_{\text{ads}} \quad (8)$$

The slope and intercept of the plot gives the values of ΔH° and ΔS° . The temperature effect of the amount of basic dye, BR46, adsorbed onto clay at various temperatures was examined. The results are shown in table 3. It can be seen that the uptake of BR46 by clay decreases with increasing temperature, which indicates that the adsorption of BR46 is controlled by an exothermic process, it is confirmed by the negative value of ΔH° . This validates the subsistence of the attractive forces weakening between dye and adsorbent sites [32]. Similar trend was observed for Chrysoidine R dye on fly ash [33]. The decrease in adsorption capacity of clay at higher temperature may be attributed to the tendency of the dye molecules to escape from the solid phase to the bulk phase with an increase in the temperature of the solution. Since the adsorption is an exothermic process, it would be expected that an increase in solution temperature would result in a decrease in

, so the adsorption of BR46 onto clay and involves a physical adsorption [34].

For the BM and the GM dyes, the adsorption is endothermic in nature since the value of ΔH is positive. The endothermic nature is also indicated by the increase in the amount of adsorption with temperature (Table 3) [12]. The adsorption is associated with an increase in entropy of $37 \text{ J mol}^{-1} \text{ K}^{-1}$ and $50 \text{ J mol}^{-1} \text{ K}^{-1}$ for the BM and the GM which shows that the adsorbed dyes molecules onto clay surface are organized in more random fashion compared to those in the aqueous phase. Similar observations have been reported in the literature [35, 36]. The higher heat of adsorption obtained in this work indicates that chemisorption rather than the physical adsorption is prevalent in this case [37].

An increase in adsorption with increase in temperature was observed, the process to be endothermic showing that the chemical adsorption of the BM and GM onto. We note also that ΔH values obtained from adsorption of BR46 onto clay are lower than that of BM and GM. This result for BR46 gives clear evidence that the interactions between BR46 and the surface hydroxyl groups of clay may be weaker than those obtained for the BM and the GM [38].

3.4. Activation parameters

With respect to the kinetic modelling, the pseudo-second order [29] model has been examined to find out the adsorption mechanism:

$$\frac{t}{q_t} = \frac{1}{k_2 q_{\text{max}}^2} - \frac{1}{q_{\text{max}}} t \quad (9)$$

Where q_t is the amount of dye adsorbed (mg g^{-1}) at time t, q_{max} is the maximum adsorption capacity (mg g^{-1}), and k_2 is the rate constant of pseudo-second-order adsorption ($\text{g mg}^{-1} \text{ min}^{-1}$). The straight-line plots of t/q_t vs. t for the second-order reactions for BR46, BM, and GM onto clay have also been tested to obtain rate parameters. k , q_{max} , and the correlation coefficient r^2 of dyes under different conditions were calculated from these plots. The correlation coefficients (r^2) found for the three dyes are 0.99. These results show that the adsorption system belongs to the pseudo second-order kinetic model.

The values of the rate constant k_2 at different temperatures listed in Table 5 were applied to estimate the activation energy of the adsorption of BR46, BM and onto clay by the Arrhenius equation [39] as follows:

$$\ln k_2 = \ln A - E_a/RT \quad (10)$$

Where k_2 is the rate constant of pseudo-second order adsorption (g/mg.min), A is the Arrhenius factor, R gas constant ($8.314 \text{ J mol}^{-1} \text{ K}^{-1}$), T absolute temperature (K). Constants k_2 were calculated for each temperature (303; 313; 323; 333 K) (Table 4). The plot of $\ln k_2$ versus $1/T$ for the adsorption of the dyes onto clay was applied to obtain the activation energy, E_a from the slope, which used to determine the type of adsorption. Activation energy for BR46 adsorption onto clay is 38 kJ/ mole. Its value between 5 and 40 kJ/mole is corresponding to physical adsorption [40]. The observed activation energy ($E_a > 42 \text{ kJ/mole}$) indicated a

chemically controlled process [41] for the adsorption of BM and GM onto clay. These results are confirmed by those of thermodynamic parameters found above.

Table 3: The thermodynamic parameters of BR46, BM and GM

BR46 (20 mg/L)					BM (24 mg/L)				GM (16 mg/L)			
T (K)	q _e (mg/g)	ΔG° (kJ/mol)	ΔH° (kJ/mol)	ΔS° (kJ/mol K)	q _e (mg/g)	ΔG° (kJ/mol)	ΔH° (kJ/mol)	ΔS° (kJ/mol K)	q _e (mg/g)	ΔG° (kJ/mol)	ΔH° (kJ/mol)	ΔS° (kJ/mol K)
.....	45.68	-5.13	35.06	-7.10				
0.002	46.35	-5.50	6.081	0.037	35.39	-7.60	8.04	0.05				
.....	47.10	-5.87	35.72	-8.10				
.....	47.96	-6.24	36.22	-8.60				

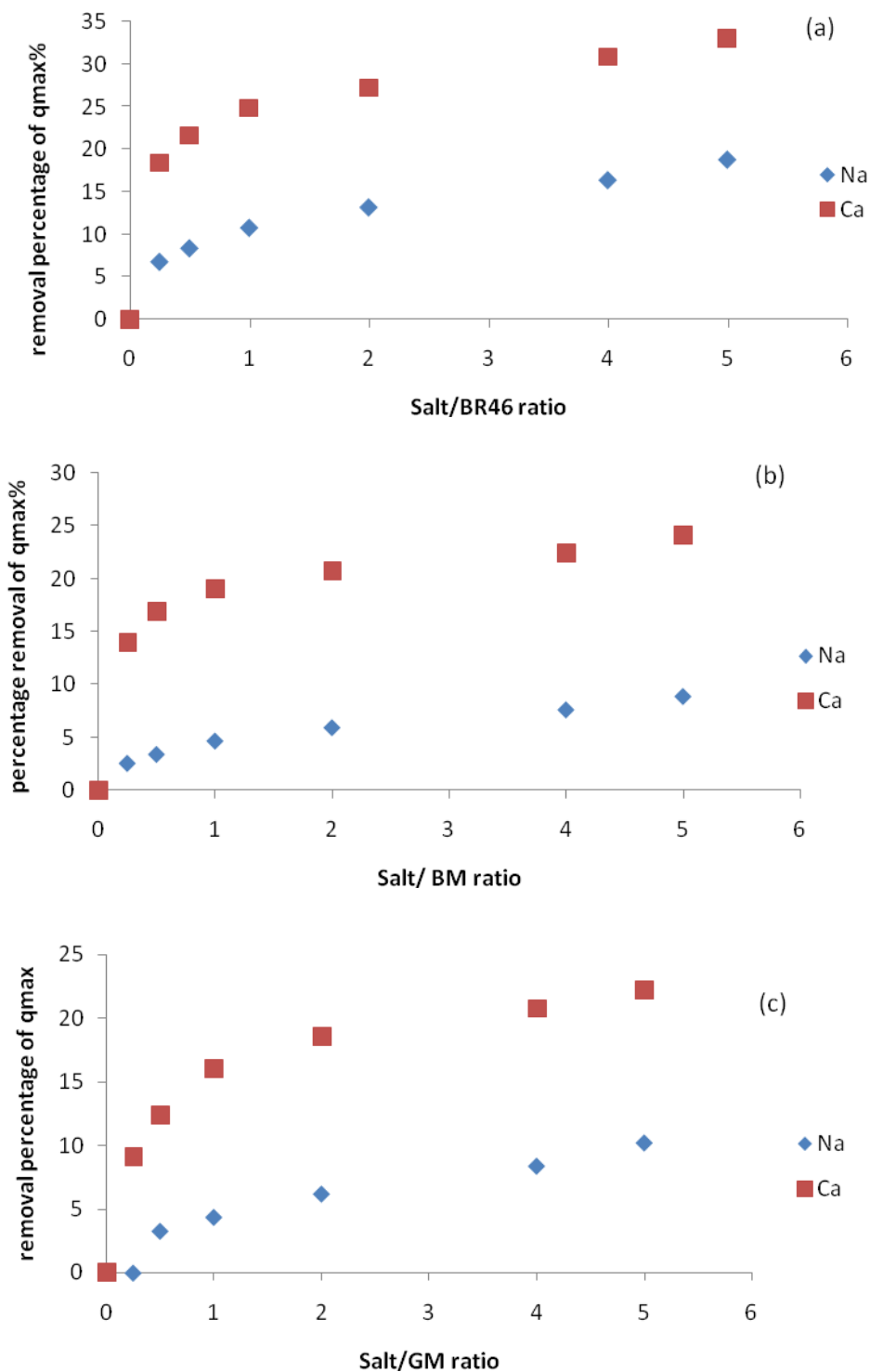
Table 4: Pseudo-second-order kinetic parameters for the adsorption of BR46, BM and GM onto clay at various temperatures

Dyes	T (K)	q _e (mg/g)	K ₂ (g/ mg.min)	R ²	E (Kj/mole)
BR46	303	40.54	0.09	0.99	39
	313	39.65	0.11	0.99	
	323	39.36	0.26	0.99	
	333	38.91	0.29	0.99	
BM	303	45.68	0.001	0.99	74
	313	46.35	0.008	0.99	
	323	47.10	0.022	0.99	
	333	47.96	0.025	0.99	
GM	303	35.06	0.013	0.99	64
	313	35.39	0.039	0.99	
	323	35.72	0.072	0.99	
	333	36.22	0.14	0.99	

3.5. Desorption studies

Wastewater streams containing dyes are generally loaded of salts, thus, the effect of salt electrolyte on BR46, BM and GM removal needs to be investigated. To clarify the role of Na⁺ and Ca²⁺ ions on the desorption phenomena, we have prepared different flask containing 50 mL of dyes clay solutions at 0.0006 M stirred until equilibrium, at which were added 50 mL of solutions containing deionized water and different volumes going from 2.5 to 50 mL of CaCl₂ and NaCl separately taken from a stock solution of 0.003 M, so, a salt dyes ratio going from 0.25 to 5. Generally, the presence of electrolyte such as NaCl, and CaCl₂ may have different effects in aqueous solution. These salts are dissociated in water to provide positive and negative ions (Na⁺, Ca²⁺ and Cl⁻). The initial dyes concentration is 6.10⁻⁴ M and the clay mass is 40 mg. The results showing calculated percentage of q_{max} removal so the desorption study in the presence of calcium or sodium ions are shown in Fig. 3. This figure shows that there was a decrease in the adsorption capacities by increasing in the concentration of salts added. However, as revealed in Fig. 3, there was a significant reduction in the adsorption of dyes so, an increase in the desorption of these dyes onto clay when the salt dye ratio is less than 1. The percentage decrease in adsorption capacity so, the percentage desorption studies was 18.8 %; 8.88 %; 10.18 % with NaCl solutions and 33 %; 24.12 %; 22.18 % with CaCl₂ solutions for BR46, BM and GM respectively. At low salt concentrations, electrostatic repulsions are predominant so that high salt retentions are obtained. The retention factor of NaCl and CaCl₂ is low when the salts concentration is high with reduction in electrostatic interactions.

This can be explained by the screening effect due to addition of NaCl or CaCl₂. Theoretically, the electrostatic forces between the adsorbent surface and adsorbate ions attractive and an increase in ionic strength will decrease the adsorption capacity [42]. Whereas, when the salt dye ratio is more than 1, limited effect is occurred (less than 10% inhibition) for the same salt concentrations about five times. This effect of ionic strength on dye ion adsorption is often attributed to the competition between positives cations of the electrolytes (NaCl and CaCl₂) and dyes ions for the surface sites, where the cations of these salts solution compete much more effectively for permanent negatively charged sites (silanol sites, Si-OH) on the kaolinite faces of the clay than on the aluminol sites (Al-OH) [43].



- **Figure 3:** Na⁺ and Ca²⁺ effect on the dyes desorption: (a) BR46, (b) BM and (c) GM (T: 25 ± 2) °C, m_{clay}: 400 mg /L)

It is also suggested that increasing salts dyes ratio can cause screening of surface negative charges by the electrolyte salts ions leading to a drop in the adsorption of the dyes ions [44-45]. Therefore, a decrease in adsorption of dyes, so, an increase in the desorption of them with increasing ionic strength of salts solutions implies that increasing ionic strength is making the potential of the adsorbent surface less negative and thus would decrease dyes ion adsorption [45, 46]. It is also observed that more dyes molecules ions were desorbed from the adsorbent in presence of CaCl_2 than dyes desorbed in the presence of NaCl (18.8 %; 8.88 %; 10.18 % with NaCl solutions and 33 %, 24.12 %, 22.18 %) with CaCl_2 solutions for BR46, BM and GM respectively (Fig. 3); Moreover, The results of the dyes ions leached from the adsorbent demonstrate that the leaching amount of divalent ions (Ca^{2+}) in all samples are significantly higher than that of univalent (Na^+). Thus, the clay surface is more enriched by the positives charges of the bivalent cations addition than by the monovalent ones and make the repulsion between the adsorbent and the cationic dye external surface easy. The effect of Na^+ and Ca^{2+} on BM and GM dyes is nearly similar. As against, there is an increase in the desorption of BR46 (Fig.3), this suggest that the interactions between BR46 and the surface hydroxyl groups of the clay may be more weak than those between BM, GM and the clay, which is confirmed by the results observed for the thermodynamics parameters and the activation energy.

3.6. IR adsorption mechanism of the BR46, BM and GM dyes.

ATR-FTIR spectra of the samples were recorded with a JASCO corp, FT/ IR 620 REV. 1.00. Spectrometer, as presented in Fig. 4.

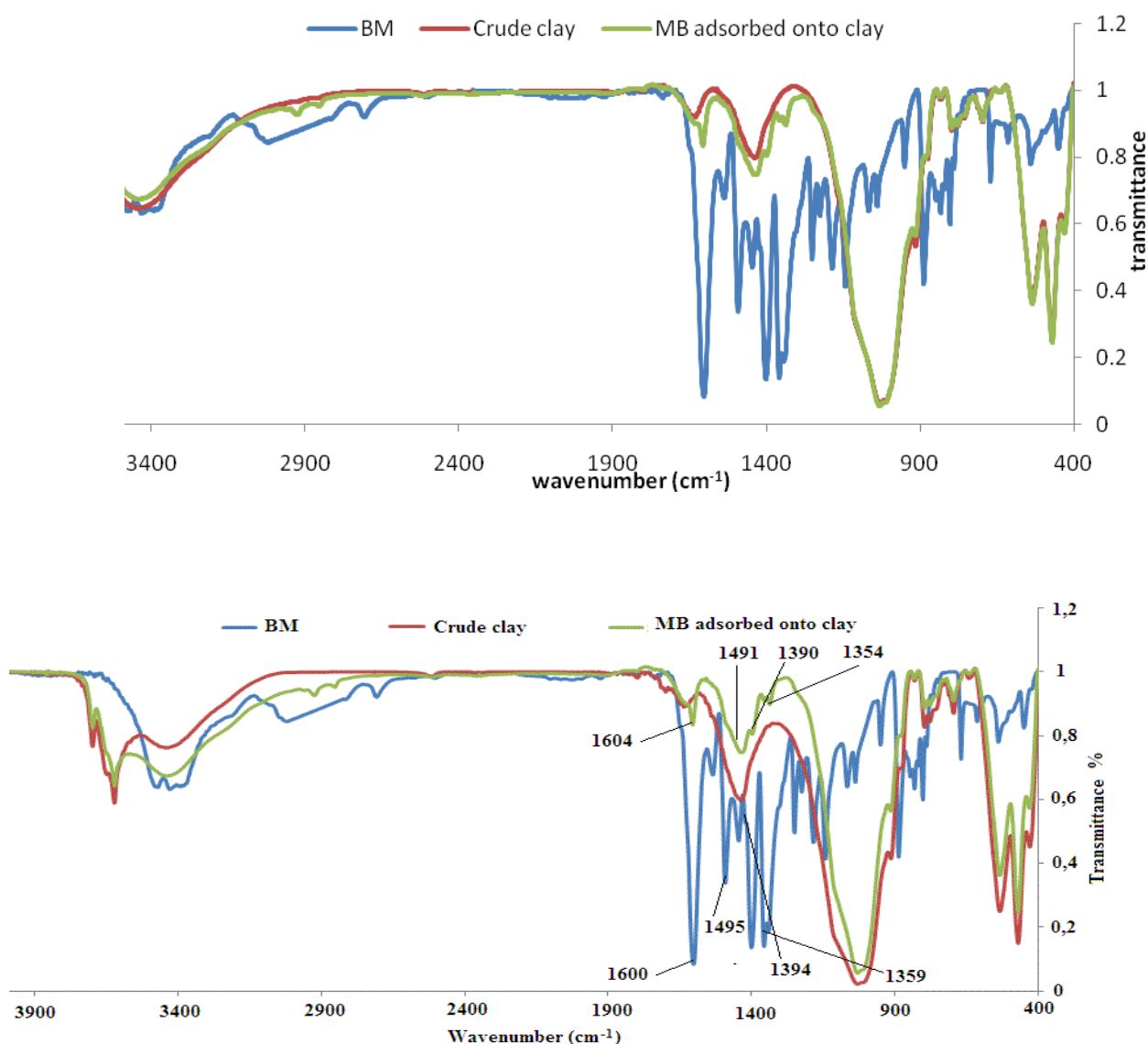


Figure 4: IR spectra of the BM dye, the raw clay and clay saturated with BM dye

All spectra were taken in the range of 4000- 400 cm^{-1} . The Fig. 4 showed the clay, the dye and the clay saturated with BM dye spectrums. The spectrum accorded to raw clay is demonstrated in section: 3.1. For the MB dye, the peak related to the vibration of the aromatic ring at 1600 cm^{-1} was very prominent. Two peaks at 1495 and 1394 cm^{-1} were recognized as the C-N stretching vibrations. The vibrations of the CH_3 group were found at 1359 cm^{-1} . The spectrum of MB adsorbed onto clay displayed in figure 4 presents a shift for the peaks corresponding to MB with the aromatic ring vibration at 1604 cm^{-1} , the C-N stretching vibrations at 1490 cm^{-1} and 1390 cm^{-1} and the CH_3 group vibrations at 1354 cm^{-1} , reflecting the evidence for the strong interaction between MB and clay (by dipole - positive charge bond, hydrogen bond between the raw clay hydroxyl groups and the free electron pair of the nitrogen in the BM molecule interactions respectively), in accordance with the low values of R_L obtained above.

Fig. 5 showed the clay, the dye and the clay saturated with GM dye spectrums. The figure representative of the GM dye shows a predominant peak related to the vibration of the aromatic ring at 1591 cm^{-1} , the peaks related to C-N stretching vibrations are seen at 1487 cm^{-1} and 1379 cm^{-1} . CH_3 is observed at 1313 cm^{-1} , the spectrum of GM adsorbed onto clay displayed in figure 5 shows a GM displacement of aromatic ring band vibration at 1610 cm^{-1} after adsorption, a shift for the C-N stretching at 1434 cm^{-1} and 1407 cm^{-1} , and a CH_3 displacement of the vibration band at 1344 cm^{-1} . This shows that the established interactions are dipole-dipole nature. For the tree cationic dyes, the displacement is observed at near than about 1600 cm^{-1} , this indicates that COOH could be the potential adsorption sites for interaction with the cationic dyes.

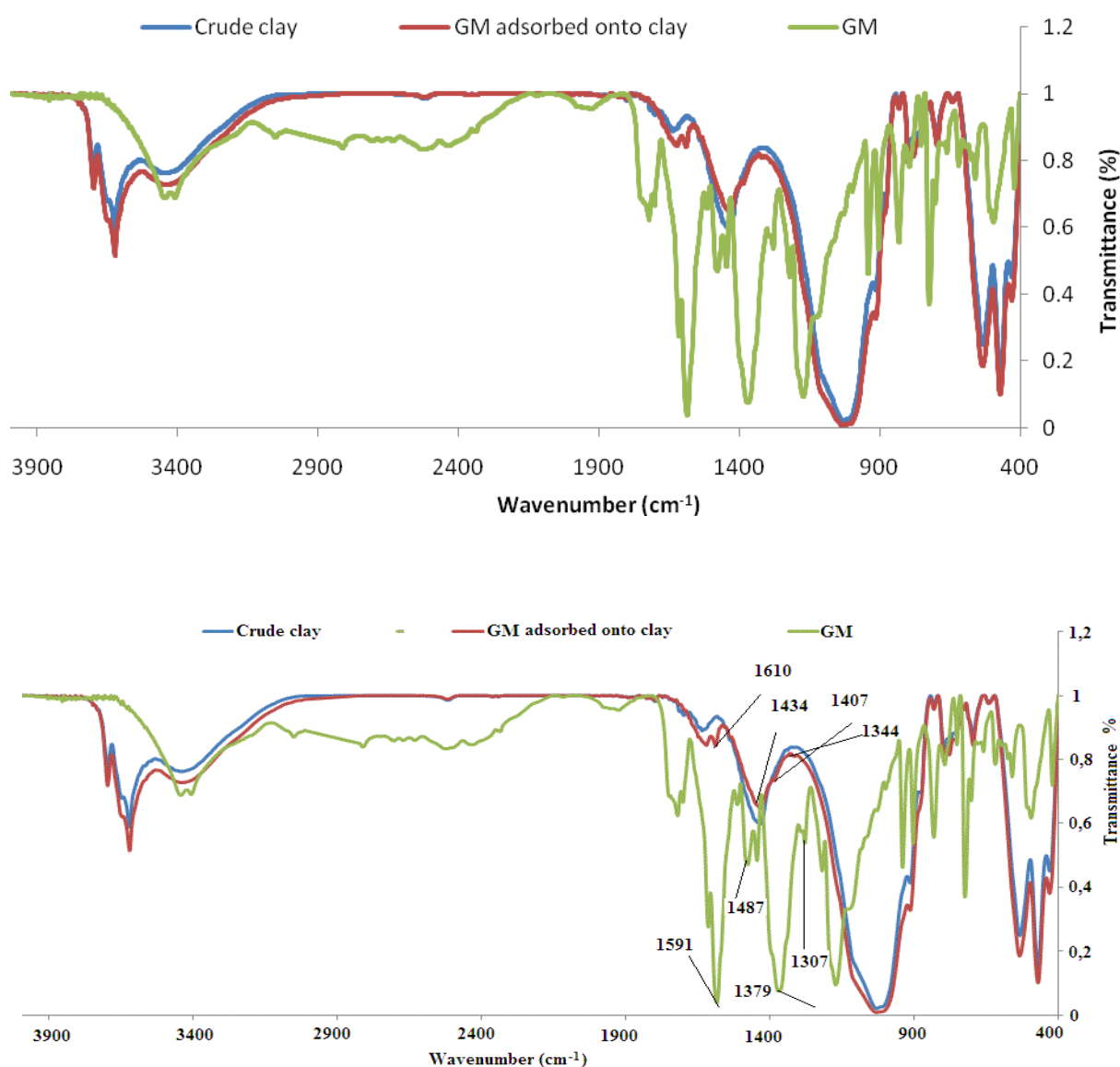


Figure 5: IR spectra of the GM dye, the raw clay and clay saturated with GM dye

Moreover, we have observed for the BM and GM, an activation energy $E_a > 42$ kJ/mole indicating a chemically controlled process [41]. This strong interaction was demonstrated by BM and GM desorption tests, we noticed that these dyes have a very low desorption.

For the BR46 dye, clay saturated by dye shown in figure 6, we observe a predominant peak at 1600 cm^{-1} related to aromatic ring, a peak at 1454 cm^{-1} related to C-N stretching vibrations and a peak at 1417 cm^{-1} for the CH_3 group, Several weak peaks between 1253 cm^{-1} and 669 cm^{-1} were ascribed to the C-H in plane and out of plane bending vibrations for the three dyes [47]. from this figure (Fig 6), we note a displacement of the vibration band at 1610 cm^{-1} , a shift at 1358 cm^{-1} reflecting lower interaction BR46 dye molecules with clay. Also, the activation energy observed for the BR46 is $E_a < 40$ kJ/mole indicating a physical controlled process [41], this is confirmed by desorption results (lower than BM and GM).

Finally, the cationic MB, BR46 en GM molecules were readily adsorbed onto negatively charged sites of the clay by charge attraction. Therefore, it was concluded that electrostatic attraction might play a major role in the initial bulk diffusion for the three dyes. This was in agreement with previous studies on the adsorption of acid blue 40 onto P25 titania [37] and hexokinase onto silicon wafers [44]. They also indicated that the adsorption was mainly driven by electrostatic forces. Similar to the reports in Ref. [46], where the MB- TNTs nanocomposite was formed when MB was adsorbed onto TNTs.

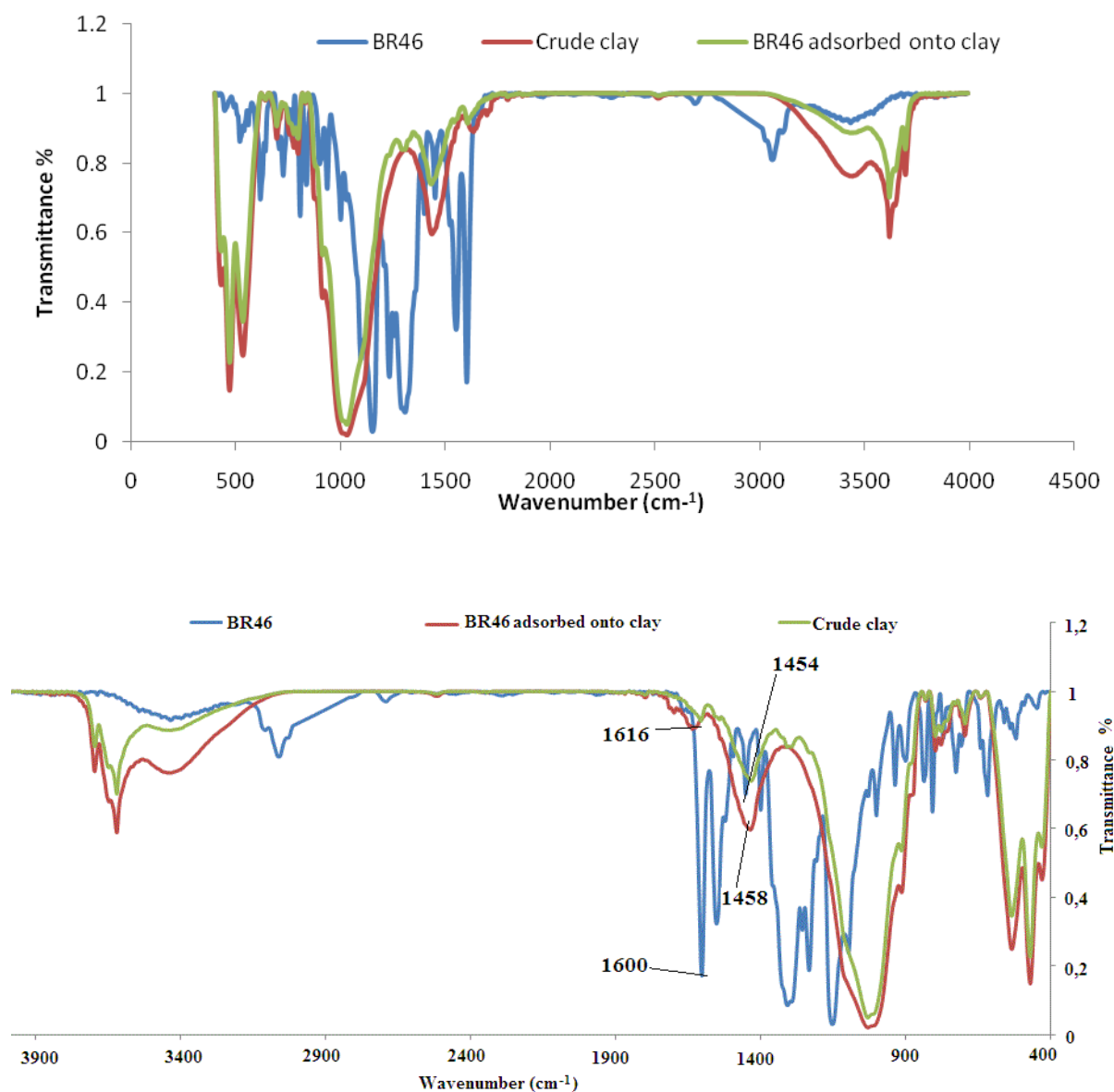


Figure 6: IR spectra of the BR46 dye, the raw clay and clay saturated with BR46 dye

Conclusion

The results in this study showed that the low cost and the abundant Moroccan clay can be used as an adsorbent for the removal of BR46, BM and GM from aqueous solution, a particular attention was paid to competitive adsorption and the effect of inorganic ions.

The sorption data indicate that Redlich Peterson equation provides better fit than Langmuir and Freundlich equation. The kinetic experiments imply that sorption process obeys the pseudo-second-order kinetic model for all pollutant studied. The temperature effect was also used to calculate the thermodynamic activation enthalpy, entropy, and free energy of adsorption. The negative value of ΔG° confirms the spontaneous nature adsorption process. The positive value of ΔS° shows the increased randomness at the solid-solution interface during adsorption. The positive value of ΔH° for GM and BM dyes indicated that the adsorption process is endothermic; the chemical nature of adsorption is occurred consequently. Whereas, it is negative for the BR46 dye, indicating the exothermic and physical processes nature. The activation energy of adsorption of BR46, GM and BM onto clay is found to be 40; 64 and 76 kJ/mole, respectively. This confirms the results found by the thermodynamics parameters (physical nature for BR46, and the chemical one for GM and BM).

The role of Na^+ and Ca^{2+} ions on the desorption phenomena of the BR46, BM and GM dyes was studied by adding to different flask containing 50 mL of dyes clay solutions at $6 \cdot 10^{-4}$ M stirred until equilibrium, 50 mL of solutions containing deionized water and different volumes of CaCl_2 and NaCl separately taken from a stock solution of 0.003 M with a salt dyes ratio going from 0.25 to 5. The results show that there is a decrease in the adsorption capacities by increasing in the concentration of salts added. However, a significant increase in the desorption of these dyes onto clay when the salt dye ratio is less than 1 was observed. Whereas, when the salt dye ratio is more than 1, limited effect is occurred (less than 10% inhibition) for the same salt concentrations about five times. It is also observed that more dyes molecules ions were desorbed from the adsorbent in presence of CaCl_2 than dyes desorbed in the presence of NaCl . These results have been confirmed by IR spectra decomposition, adsorption mechanism can be ascribed to chemical sorption for the BM and the GM, physical for the BR46 and electrostatic attraction might be predominant in the initial bulk diffusion.

In conclusion, Moroccan clay of the Safi adsorbent shows:

- A good potential for the removal of cationic dyes.
- Its use as an adsorbent for the wastewater treatment loaded with textile dyes is promoted by its natural abundance and ease of use.
- A low desorption percentage promoting the use of clay saturated with dyes in the ceramics industry and decoration products, so, an increase and a development of the Safi city economy.

Acknowledgements: We thank all the staff and professors for all the effort they made to achieve this work.

References

1. Benkhaya S., EL harfi A., *Mor. J. Chem.* 5 N°1 (2017) 1-15
2. Lakdioui T., El Harfi A., *Maghr. J. Pure & Appl. Sci.*, 2 N° 1 (2016) 25- 31
3. Jeon S. Y., Jing L., Heung Kim J., *J. Indust. and Engin. Chem.* 14 (2008) 726-731.
4. Bulut E., Özacar M., AyhanSengil I., *Microp. and Mesop. Mater.* 115 (2008) 234-246.
5. Tahir S.S., Rauf N., *Chemosphere* 63 (2006) 1842-1848.
6. Dogan M., Alkan M., Türkyilmaz A., Özdemir Y., *J. Hazard. Mater.* B 109 (2004) 141-148.
7. Bekçi Z., özveri C. Yoldas S., Yurdakoç K., *J. Hazard. Mater.* 154 (2008) 254-261.
8. Ghosh D., BhattacharyyaK.G., *Appl. Clay Sci.* 20 (2002) 295-300
9. Rais Z., Taleb M., Sfaira M., Filali Baba M., Hammouti B., Maghnouj J., Hadji M., *Phys. Chem. News*, 38 (2007) 106-111.
10. Rais Z., EL Hassani L., Maghnouj J., Hadji M., Ibn alkhayat R., Nejjar R., Kherbecheet A., Chaqroune A., *Phys. Chem. News* 7 (2002) 100-109.
11. Anirudhan T.S., Suchithra P.S., Radhakrishnan P.G., *Appl. Clay Sci.* 43 (2009) 336-342
12. Önal Y., Akmil-Basar C., Sarici-Özdemir Ç. *J. Hazard. Mater.*146 (2007) 194-203.
13. Kumar K.V., Porkodi K., *Dyes and Pigments* 74 (2007) 590-594.
14. Veli S., AlyÜz B., *J. Hazard. Mater.* 149 (2007) 226-233.

15. Bennani K.A., Mounir B., Hachkar, M., Bakasse, M., Yaacoubi, A. *J. Hazard. Mater.* 168 (2009)304-309.
16. S.Tighadouini , S. Radi, *Arab. J. of Chem. and Environ.Resear..2* N°1 (2015) 1-14
17. Ahmad M.A., NurAzreen A. P., Olugbenga S. B., *Wat. Resour. and Indust.* 6 (2014) 18-35
18. Huang J., Yuanfa L., Qingzhe J., Xingguo W., Jun Y.; *J. Hazard. Mater.* 143 (2007) 541-548
19. Madejová J, FTIR techniques in clay mineral studies, *Vibrational Spectroscopy*, 31,1, (2003),1-10
20. Brindley G.W., Susuki T., Thiry M., *Bull. Mineral.*, 106, (1983) 403-410
21. Kunquan Li, Xiaohua Wang, *Bioresour. Technol* 100 (2009) 2810-2815.
22. Cheung W.H., Szeto Y.S., McKay G., *Bioresour. Technol.* 100 (2009) 1143-1148.
23. Langmuir, I., *J. Am. Chem. Soc.* 40, (1918) 1361-1367.
24. Özcan S. and Özcan A., *J. Colloid Interf. Science* 276 (2004) 39-46.
25. Freundlich, H.M.F., *J. Physics and Chemistry* 57, (1906) 385-470.
26. Redlich, O., Peterson, D.L., *J. Physic. Chem.* (1959).63, 1024.
27. Giles C.H., Mac Evan T.H., Nakhwa S.N., Smith D., *J. Chem. Soc.* 111 (1960) 3973-3993.
28. Giles C.H.,Silva A.P.D, Easton I.A., *J. Colloid Interface Sci.* 47 (3) (1974) 766-778.
29. Özcan S. A., Bilge Erdem, Adnan Özcan, *J. Colloid and Interf. Sci.* 280 (2004) 44-54
30. Mohd A., NurAzreen A. P., Olugbenga S. B., *Wat. Res. and Ind.* 6 (2014)18-35.
31. Bakas I., Elatmani K., Qourzal S., Barka N., Assabbane A., Aît-Ichou I., *J. Mater. Environ. Sci.* 5 (3) (2014) 675-682.
32. Singh D., *Ads..Sci. Technol.* 18 (8) (2000) 741.
33. Matheswaran M., Karunanithi T., *J. Hazard. Mat.* 145 (2007) 154-161
34. Panday K.K., Prasad G., Singh V.N., *J. Chem. Technol. Biotechnol.A* 34 (1984) 367.
35. Bhattacharyya K.G., Sarma A., *Dyes Pigments* 57 (2003) 211- 222.
36. Purkait M.K., Maiti A., Das Gupta S., De S., *J. Hazard. Mater.* 145 (2007) 287-295
37. McKay G. (Ed.), CRC Press, New York, (1996).
38. Ugurlu M. *J. Microp. and Mesop. Mat.* 119, (2009) 276-283.
39. Septum C. et al. *J. Hazard. Mat.* 148 (2007) 185-191
40. Wu C-H, *J. Hazard. Mat.* 144 (2007) 93- 100
41. Weng C.H., Pan Y.F., *J. Hazard. Mater.* 144 (2007) 355-362.
42. Malekbala M.R., Moonis A. K., Soraya H., Luqman C. Abdullah Thomas S.Y. Choong, *J. Ind. and Eng. Chem.* 21 (2015) 369-377.
43. Spark K.M., Wells J.D., Johnson B.B., *Eur. J. Soil Sci.* 46 (1995) 633-640.
44. Coles C.A., Yong R.N., *Appl. Clay Sci.* 22 (2002) 39-45.
45. Unuabonah E.I., Adebowale K.O., Olu- Owolabi B.I., Yang L.Z., Kong L.X. *J. Hydrometallurgy*, 93 (2008) 1-9
46. Jiang M. Xiao-ying Jin, Xiao-Qiao Lu, Zu-liang Chen, *Desalination* 252 (2010) 33-39
47. Yan Y.M., Zhang M.N., Gong K.P., Su L., Guo Z.X., Mao L.Q., *Chem. Mater.*17 (2005) 3457-3463.

(2017) ; <http://www.jmaterenvironsci.com>